Eur. Phys. J. A **24**, 23–29 (2005)
DOI 10.1140/epja/i2004-10120-y

THE EUROPEAN PHYSICAL JOURNAL A

First evidence for chirality in Tc isotopes: Spectroscopy of ^{100}Tc

P. Joshi[1,a], A.R. Wilkinson[1], T. Koike[2,b], D.B. Fossan[2], S. Finnigan[3], E.S. Paul[3], P.M. Raddon[1], G. Rainovski[2,3,c], K. Starosta[4], A.J. Simons[1], C. Vaman[2], and R. Wadsworth[1]

[1] Department of Physics, University of York, Heslington, York YO10 5DD, UK
[2] Department of Physics and Astronomy, SUNY at Stony Brook, Stony Brook, NY 11794-3800, USA
[3] Department of Physics, University of Liverpool, Liverpool L69 7ZE, UK
[4] Department of Physics and Astronomy, Michigan State University, 164 S. Shaw lane, East Lansing, MI 48824-132, USA

Received: 17 November 2004 / Revised version: 20 December 2004 /
Published online: 28 January 2005 –
Communicated by D. Schwalm

Abstract. Excited states in ^{100}Tc have been studied using the ^{96}Zr(^{7}Li, 3n) reaction at a beam energy of 27 MeV. In the present work, evidence has been found for a second $\Delta I = 1$ band decaying via several stretched dipole transitions to the previously known $\Delta I = 1$ negative-parity band. Comparison of these data with those in neighbouring nuclei and also against recently reported criteria for chiral bands in nuclei, suggests that the two structures can be interpreted as chiral partners. Core quasi-particle coupling model calculations show reasonable agreement with the data and generally support the chiral interpretation of the states.

PACS. 21.10.Re Collective levels – 21.60.-n Nuclear structure models and methods – 23.20.Lv γ transitions and level energies – 27.60.+j $90 \leq A \leq 149$

1 Introduction

The first predictions of chiral effects in triaxial nuclei were made by Frauendorf and Meng in 1997 [1]. This work was further supplemented by Dimitrov *et al.* [2] who showed that chiral symmetry can be spontaneously broken in the rotating mean field of a triaxial odd-odd nucleus. This phenomenon results in two nearly degenerate $\Delta I = 1$ bands from the left-handed and right-handed solutions. Chirality was predicted to result from the coupling of high-j proton (neutron) particles and high-j neutron (proton) holes with the rotational angular momentum vector, $\mathbf{R}$. The high-j particle-like orbits have their angular momentum vector oriented along the short axis of the triaxial core whilst for the high-j hole-like orbits the vector is oriented along the long axis. The collective angular momentum vector of the core lies along the intermediate axis of the triaxial nucleus since this has the largest moment of inertia for irrotational-like flow, and consequently minimises the rotational energy.

The first experimental evidence for chiral structures, based on a $\pi h_{11/2} \otimes \nu h_{11/2}^{-1}$ configuration, was reported in several $N = 75$ isotones in the mass-130 region, with the best example of chiral rotation, in terms of energy degeneracy, occurring in ^{134}Pr [3,4]. This work also revealed that for many of the $N = 75$ nuclei the doublet bands did not become completely degenerate. Instead there was a small, but almost constant, energy difference between the bands. This was interpreted as evidence for collective chiral vibrations. The latter effect results when any imperfections in the formation of the chiral geometry are not negligible. For instance, the core is not stable at around $\gamma = 30°$ but is more γ-soft, thus allowing the rotational angular momentum vector $\mathbf{R}$ to oscillate from one chiral system to the other, *i.e.* to tunnel through the energy barrier in the plane spanned by the short-long axes of the triaxial shape. A vibration of $\mathbf{R}$ between the left- and right-handed chiral systems is very similar to the well-known phenomenon of collective octupole vibration that is observed between reflection asymmetric shapes. The observation of chirality in nuclei is important, since it provides direct evidence for triaxial shapes, which has been a long sought after goal in nuclear-structure physics.

Since the first experimental results were reported in the $A = 130$ region, there have been many other examples of similar structures observed in this mass region, *e.g.* see [5–10]. These provide support for the existence of a small island of chiral structures, centred on ^{134}Pr. The work of Dimitrov *et al.* [2] indicated that chiral bands may

[a] e-mail: pj9@npg.york.ac.uk
[b] *Present address*: Department of Physics, Tohoku University, Sendai 980-8578, Japan.
[c] Presently on leave from the Faculty of Physics, St Kliment Ohridski University of Sofia, 1164 Sofia, Bulgaria.

be found in other regions of the Segre chart. In particular, they predicted a region of chiral rotors to exist in the odd-odd Ir nuclei around $A \sim 188$. Recent experimental work in this region has provided the first evidence for such structures in ^{188}Ir [11]. However, the majority of the recent experimental work has centred on nuclei in the $A \sim 100$ region. Here, Vaman *et al.* have found evidence for what currently appears to be the best case of chiral rotation found to date [12]. This work was initially reported in ref. [13], where a detailed theoretical investigation of the expected properties of chiral structures was also carried out for the mass-130 region and some general conclusions were made. This work revealed three fingerprints for such structures, which can be summarised as follows: a) there should be near degenerate doublet $\Delta I = 1$ bands (*i.e.* having the same spins and parities) over a range of spins I, b) the parameter $S(I) = [E(I) - E(I-1)]/2I$ for these bands should vary smoothly with spin, *i.e.*, there should be no staggering, and c) there exists $M1$ and $E2$ selection rules as a result of restoration of the chiral symmetry in the laboratory reference frame as a function of spin, I. Detailed theoretical investigations indicate that the latter feature results in a staggering of the $B(M1)/B(E2)$ ratios for the two chiral bands. Furthermore, the chiral symmetry restricts the phase of this staggering such that for odd- (even-) parity configurations the even (odd) spins should have high values and odd (even) spins should have low values. A similar staggering, with the same phase, should also be observed in the $B(M1)_{\rm in}/B(M1)_{\rm out}$ ratios for these bands. Further evidence for a new region of chirality around mass 104 has recently been found in the odd-odd isotopes ^{102,106}Rh [14,15] and also in the odd-mass neighbour ^{105}Rh [16]. The present work on ^{100}Tc, which is an isotone of ^{102}Rh, provides the first indication that this region extends beyond the Rh isotopes. The new data on ^{100}Tc will be compared with both the theoretical expectations discussed above and the results of core quasi-particle coupling model calculations.

2 Experimental method and data analysis

The ^{96}Zr(^{7}Li, 3n) reaction was used to populate states in ^{100}Tc at a beam energy of 27 MeV. The ^{7}Li beam was produced from the tandem accelerator at the State University of New York at Stony Brook. γ-rays from the reaction products were detected using an array of six Compton suppressed HPGe detectors and a 14-element BGO inner-ball calorimeter. A good event required two suppressed γ-rays in the Ge detectors in coincidence with at least two events detected in the BGO inner ball. The target used was 1.2 mg/cm^2 of 85% enriched ^{96}Zr on a 20 mg/cm^2 lead backing. Since the present work used the strong 3n channel from the ^{7}Li + ^{96}Zr reaction, additional gating on the fold, K, or on the sum energy, H, in the BGO multiplicity filter did not produce a significant improvement in the quality of the spectra; therefore, no further filters on either of these parameters were implemented in the final data analysis.

Data were stored on exabyte tapes for off-line analysis. The sources ^{133}Ba and ^{152}Eu were used to calibrate the energy and to measure the relative efficiency of the Ge detectors. The gain-matched data were sorted into an E_γ-E_γ matrix and analysed using the ESCL8R Radware software package [17] in order to produce a partial decay scheme for ^{100}Tc. In addition to this, a directional correlation from oriented states (DCO) [18] analysis was also carried out using the γ-γ coincidence data between detectors at forward and backward angles ($\theta_{\rm eff} = 34^\circ$) and those placed at 90°. In this case an E_γ-E_γ matrix was sorted which had detectors located at 90° to the beam direction on the y-axis and the forward/backward detectors on the x-axis. The DCO ratio measured is defined as

$$R_{\rm DCO}(E_\gamma) = \frac{I_{34}(E_\gamma)}{I_{90}(E_\gamma)} \,, \tag{1}$$

where $I_{90}(E_\gamma)$ and $I_{34}(E_\gamma)$ are the intensities of a transition E_γ as seen in a 90° detector and 34° detector when gated by a γ-transition of a given multipolarity at the angles 34° and 90°, respectively. For this geometry DCO values of 1 are expected for a stretched quadrupole (dipole) transition when the gating transition is also a stretched quadrupole (dipole) transition, whilst a value of 0.5 (or 1.85) is expected for a stretched dipole (quadrupole) if the gating transition is a stretched quadrupole (dipole). These values were confirmed by gating on known $E2$ and $E1$ transitions in ^{99}Tc [19] and ^{100}Tc [20]. The intensities of the γ-rays allowed us to measure the $B(M1)/B(E2)$ ratios for the transitions of the yrast band and the $B(M1)_{\rm in}/B(M1)_{\rm out}$ values for the transitions de-exciting the levels of the new partner band. These data were extracted using the following expressions:

$$\frac{B(M1)_{\rm in}}{B(M1)_{\rm out}} = \frac{E^3_\gamma({\rm out})}{E^3_\gamma({\rm in})} \frac{\lambda_{\rm in}}{\lambda_{\rm out}} \,, \tag{2}$$

$$\frac{B(M1)}{B(E2)} = 0.697 \frac{E^5_\gamma(E2)}{E^3_\gamma(M1)} \frac{\lambda_{M1}}{\lambda_{E2}} \,, \tag{3}$$

where λ represents the intensity of the transition and only small $E2$ mixing for the $\Delta I = 1$ transitions (mixing ratio $\delta^2 \sim 0$) is assumed.

3 Results and discussion

Previous work on ^{100}Tc [20] had established excited states up to spin 14 in the yrast negative-parity band. Figure 1 shows the partial decay scheme deduced from the present work, whilst table 1 summarises the γ-ray energies, intensities, DCO ratios and the assigned multipolarities. The relative γ-ray intensities listed are normalised to the intensity of the 300 keV transition in the yrast band (band A). The yrast level scheme has been extended up to the $I^\pi = 16^-$ state (tentatively, 17^-) while a new excited band (band B), connected to the yrast band through $M1/E2$ transitions, has been observed up to the tentatively assigned 15^- state. This new band consists mainly

Table 1. Spins, parities, γ-ray energies (in keV), γ-ray intensities and $R_{\rm DCO}$ values for transitions in ^{100}Tc from the present work.

J_i^π	E_γ	I_γ	$R_{\rm DCO}$	Multipolarities
3^+	91.4	5.3(2)		$(M1/E2)$
8^-	99.0	88.5(3)		$M1/E2$[a]
5^-	105.7	28.7(2)		$(E1)$
6^-	144.2	35.2(1)		$(M1/E2)$
2^+	172.1	27.3(10)		$M1/E2$[a]
6^-	225.3	77.3(4)		$E1$[a]
11^-	251.5	64.7(2)	0.94(1)[d]	$M1/E2$
3^+	263.5	19.0(10)		$E2$[a]
6^-	300.4	100.0(5)		$E1$[a]
12^-	338.9	3.9(1)		$(M1/E2)$
10^-	377.1	78.6(2)	1.02(13)[h]	$M1/E2$
13^-	398.4	19.0(1)	0.40(4)[b]	$M1/E2$
			0.97(6)[d]	$M1/E2$
13^-	407.7	0.63(4)		$(M1/E2)$
(15^-)	419.6	0.43(3)		$(M1/E2)$
12^-	433.6	48.7(1)	0.48(4)[b]	$M1/E2$
			0.93(23)[d]	$M1/E2$
10^-	446.9	0.34(5)		$(E2)$
14^-	455.1	18.5(1)	0.94(4)[d]	$M1/E2$
(14^-)	471.1	1.53(5)		$(M1/E2)$
11^-	472.2	2.89(6)	1.09(13)[e]	$M1/E2$
16^-	478.9	2.6(1)		$(M1/E2)$
15^-	540.6	3.1(1)	0.85(14)[c]	$M1/E2$
11^-	629.0	42.6(2)	1.53(14)[h]	$E2$
(17^-)	644.4	1.02(5)		$(M1/E2)$
12^-	685.6	6.1(1)	1.53(5)[d]	$E2$
13^-	(743)			$(E2)$
10^-	804.5	9.0(1)	1.02(12)[h]	$M1/E2$
12^-	809.7	1.88(6)	1.49(24)[e]	$E2$
13^-	832.7	31.4(1)	0.97(4)[b]	$E2$
14^-	853.8	9.68(7)	0.86(16)[f]	$E2$
11^-	898.3	10.53(8)	1.07(5)[d]	$M1/E2$
13^-	956.9	6.45(6)	0.47(9)[b]	$M1/E2$
12^-	986.1	4.92(7)	0.50(10)[b]	$M1/E2$
15^-	995.2	7.81(8)	0.96(23)[b]	$E2$
(15^-)	996.9	3.06(7)		$(M1/E2)$
16^-	1014.7	5.94(6)	1.18(11)[c]	$(E2)$
(14^-)	1030.5	1.02(4)		$(M1/E2)$
(17^-)	1125.1	1.53(4)	1.13(17)[g]	$E2$
12^-	(1236.7)			$(E2)$

[a] From previous work;
[b] gate on 629 keV ($E2$);
[c] gate on 455 keV ($M1/E2$);
[d] gate on 377 keV ($M1/E2$);
[e] gate on 805 keV ($M1/E2$);
[f] gate on 686 keV ($E2$);
[g] gate on 629 and 833 keV ($E2$'s);
[h] gate on 225 keV ($E1$).

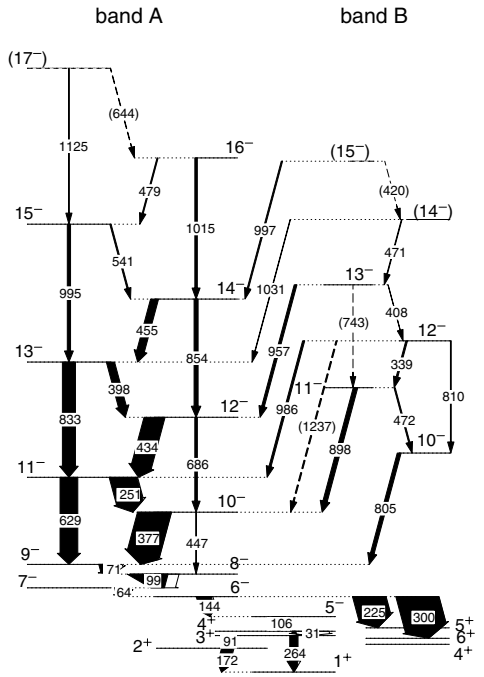

Fig. 1. Partial level scheme of ^{100}Tc, deduced from the present work.

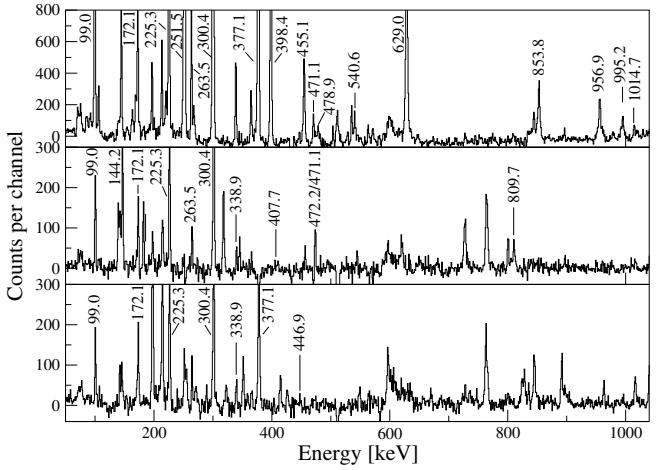

Fig. 2. Experimental spectra showing the inter-band transitions and the evidence for linking transitions from the new side band to the yrast band in ^{100}Tc. Top, middle and bottom spectra correspond to gates on 434.0 keV, 804.5 keV and 898.3 keV transitions in ^{100}Tc, respectively.

of the inter-band $M1$ transitions, which indicates that the interconnecting $E2$ transitions are weak (only one such transition, 810 keV, between the 12^- and 10^- states has been observed in the present experiment). Figure 2 shows a selection of γ-ray spectra in support of the proposed decay scheme. The extracted DCO ratios for the connecting intra-band transitions are consistent with these γ-rays having a predominantly stretched dipole character. Comparison with similar structures in the odd-odd Rh isotopes (see below) suggests that these are magnetic dipole

transitions, thereby indicating that the parity of this band is the same as that of the yrast band.

Recent work in ^{102,104,106}Rh [12,14,15] has revealed the presence of pairs of strongly coupled negative-parity structures in all three nuclei. In ^{104}Rh three strong intraband linking transitions were found to have DCO ratios consistent with stretched dipole transitions. Furthermore, a linear polarisation measurement of one of these transitions confirmed that it has magnetic character. This latter feature essentially proved that both of the doublet bands must have the same configuration [12] (containing two unique-parity orbitals), since transitions between this and any other possible configuration would have to involve a change of both of the occupied orbitals if the parity is not to change in such a transition. Such a scenario is not allowed because $M1$ and $E2$ electromagnetic transitions involve one-body operators, *i.e.*, only one orbital can change when such transitions occur. In ^{104}Rh the two bands have been assigned a $\pi g_{\frac{9}{2}}^{-1} \otimes \nu h_{\frac{11}{2}}$ configuration based on the properties of the bands and a g-factor measurement of the band-head state in the yrast band. Following detailed theoretical studies, the negative-parity bands found in the ^{104,106}Rh nuclei were interpreted in terms of chiral structures. The two structures observed in ^{100}Tc appear to be very similar to those observed in ^{102,104,106}Rh [12,14,15] (^{102}Rh is an isotone of ^{100}Tc); furthermore, previous work on ^{100}Tc has already assigned a $\pi g_{\frac{9}{2}}^{-1} \otimes \nu h_{\frac{11}{2}}$ configuration to the negative-parity yrast band. Thus, using the above information together with the experimental DCO ratios for the states connecting the two structures, we tentatively assign the same configuration to the new side band in ^{100}Tc.

It is interesting to note that in ^{100}Rh similar negative-parity structures were observed some time ago [21]. In this case, a different explanation was put forward for the second strongly coupled structure. It was tentatively suggested that it might involve the $\pi p_{\frac{1}{2}}^{-1} \otimes \nu\left(g_{\frac{7}{2}} d_{\frac{5}{2}}\right)$ configuration. However, given that the yrast negative-parity structure had already been assigned a $\pi g_{\frac{9}{2}}^{-1} \times \nu h_{\frac{11}{2}}$ configuration, this seems very unlikely when bearing in mind the comments above on the one-body nature of the electromagnetic operators. Furthermore, we note that the ^{100}Rh work was only a short paper and had no detailed theoretical basis for the proposed structure. Moreover, at the time of that work the existence of chiral bands was unknown. It would therefore seem reasonable to suggest that the negative-parity bands observed in ^{100}Rh may also be interpreted in terms of a chiral picture.

3.1 Tests for chirality

The introduction summarises three key signatures for chirality in nuclei which have arisen from recent theoretical work [12,9]. In this section the results for ^{100}Tc will be compared against these criteria. The top part of fig. 3 shows the excitation energy *vs.* spin for the two structures observed in ^{100}Tc along with data for similar bands

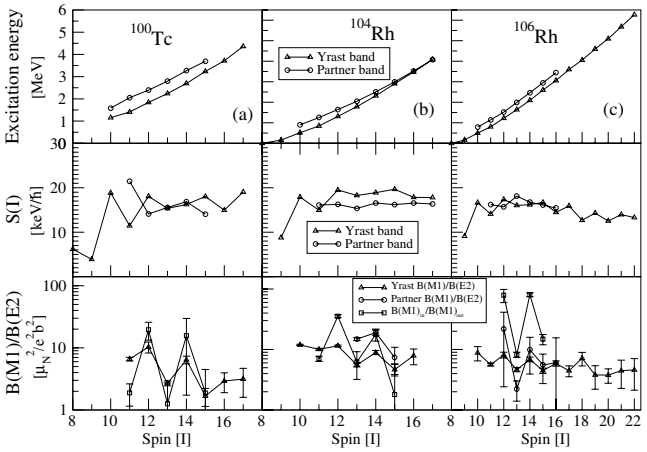

Fig. 3. A comparison of the three characteristic signatures of chirality in $A \sim 100$ mass region. The panels (a), (b) and (c) correspond to ^{100}Tc, ^{104}Rh and ^{106}Rh, respectively, while the top, middle and the bottom parts show the energy, $S(I)$ (defined as $S(I) = [E(I) - E(I-1]/2I)$ and the $B(M1)/B(E2)$ ratios for the yrast and the partner bands along with the $B(M1)_{\rm in}/B(M1)_{\rm out}$ ratios. The $B(M1)/B(E2)$ ratios for the partner band in ^{100}Tc are not shown since crossover $E2$ transitions were not observed.

in ^{104,106}Rh. It is clear that ^{100}Tc has a very similar behaviour to ^{106}Rh in that it does not achieve the energy degeneracy seen in ^{104}Rh. The energy gap between the two bands in ^{100}Tc is approximately constant at ~ 550 keV in the spin 10 to 14 range. Similar behaviour was observed in the neighbouring isotopes and isotones of ^{134}Pr, where the magnitude of energy gap between the two structures typically ranges from ~ 150 keV to ~ 400 keV. We note, however, that in ^{124}La [22] the two chiral-like bands have an energy gap ~ 500 keV between them.

An explanation for the lack of degeneracy may be that the triaxial deformation is not stable, but somewhat γ-soft. This would result in the rotational angular momentum vector spending some time in the plane of the short-long axes in addition to being perpendicular to that plane. This could give rise to the phenomenon of chiral vibrations as discussed in ref. [4].

The middle part of fig. 3 shows a comparison of the $S(I)$ parameter as a function of spin for the present data and the chiral structures recently identified in ^{104,106}Rh. Clearly, beyond spin 10–12, $S(I)$ shows a relatively smooth variation as a function of spin and for both bands a similar magnitude is observed in each case, as expected. The bottom part of fig. 3 shows the behaviour of the $B(M1)/B(E2)$ ratio for the yrast band states in ^{100}Tc and the $B(M1)_{\rm in}/B(M1)_{\rm out}$ ratio for the partner band. Unfortunately, the statistics were too low to enable us to identify more than one of the $E2$ transitions within the side band. This is very similar to what was observed in ^{102}Rh from a similar Stony Brook experiment [14]. More recently, a higher statistics experiment using GAMMASPHERE has revealed the presence of the missing $E2$ transitions in the side band of ^{102}Rh. Figure 3 also contains similar data for the chiral bands in ^{104,106}Rh. The ratios

clearly show a staggering which is in phase in these nuclei. It is interesting to note that the phase of the staggering is opposite to that observed in the mass-130 region. This results from the fact that the configuration now involves a $g_{9/2}$ rather than an $h_{11/2}$ proton.

3.2 Theoretical calculations

3.2.1 Woods-Saxon shape calculations

It is likely from the above observation that ^{100}Tc may have a planar component of the rotational angular momentum admixed with a non-planar, chiral component. It is also apparent from the above discussion that ^{100}Tc possesses bands with the characteristics expected for the chiral phenomena. The theoretical results showing the chiral symmetry breaking in a triaxial nucleus using the quasi-particle plus rotor model are discussed below. However, in this subsection we would first like to discuss the shape of the ^{100}Tc nucleus as deduced from Total Routhian Surface (TRS) calculations based on the Woods-Saxon (WS) potential. Similar calculations in the past have correctly reproduced the triaxial nature of the nuclear shape in the $A \sim 130$ region and have also inspired the present as well as several other studies in the $A \sim 100$ region. These calculations used a triaxial WS mean-field potential as the long-range part of the nuclear Hamiltonian, while the BCS-type short-range interaction was used between the pairs of like nucleons. The energy levels calculated in such a rotating mean field were then used to calculate the shell corrections based upon the Strutinsky procedure. These were then added to the macroscopic energy in order to obtain the total Routhian energy surface. The details of the procedure are discussed thoroughly in refs. [23,24]. The calculation was performed using a β-γ mesh while the energy was minimised at each point against the hexadecapole degree of deformation. The resulting TRS surface for the ^{100}Tc nucleus is shown in fig. 4 for four different rotational frequencies ($\hbar\omega = 0, 150, 300, 450$ keV). The figures clearly show that the nucleus should have a triaxial minimum at $\beta \sim 0.22, \gamma \sim -30°$. These results point to the triaxial nature of the ^{100}Tc nucleus and therefore, support the idea that the two bands seen in this nucleus are indeed a pair of chiral bands. The deformation parameters obtained from these calculations were used as the input to the shape of the triaxial rotor mean field in the quasi-particle plus rotor model (QPRM) calculations described below.

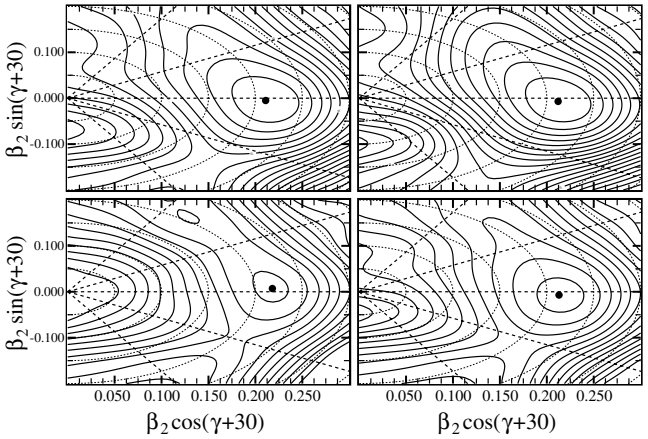

Fig. 4. The TRS calculations for ^{100}Tc for the lowest negative-parity and positive-signature configuration at four different rotational frequencies ($\hbar\omega = 0$ (bottom-left), 150 (bottom-right), 300 (top-left), 450 keV (top-right)).

3.2.2 Quasi-particle plus rotor model calculations

The quasi-particle plus rotor model [13,25,26] provides a powerful tool for studying the phenomenon of spontaneous symmetry breaking in a triaxial nucleus in the laboratory reference frame, since it enables us to calculate the electromagnetic transition strengths within the bands as well as those existing between bands. Using this model we have calculated the energies of the levels of the yrast and side bands and also the transition probabilities for the $E2$ and $M1$ transitions between the levels within these bands. In these calculations, the shape of the mean field was assumed to be a rigid rotor with the deformation of $\beta = 0.22, \gamma = -30°$ as predicted by the WS-TRS calculations mentioned above. An odd proton hole in the $g_{9/2}$ subshell and an odd neutron particle in the $h_{11/2}$ subshell were coupled to this triaxial core. The coupling constant was calculated by reproducing the correct level sequence in the nearby odd Tc isotopes. The same value of coupling constant was used for both the odd proton and neutron. The core's rotational energies were calculated using the Variable Moment of Inertia model [27] with the value of $E(2)^+ = 275$ keV used for calculating the ground-state moment of inertia. Monopole pairing between pairs of like nucleons was used as the short-range interaction. The monopole pairing constant $\Delta = 1.35$ MeV was used for both protons and neutron pairs. This was calculated using the assumption $\Delta = 135/A$. Neutron-proton pairing was not included in the calculations. The Fermi levels for the protons and neutrons were fixed so as to reproduce the correct levels in ^{99}Tc and ^{100}Tc.

Figure 5 shows the results of this calculation. The top right part of the figure shows the energy of the calculated levels as a function of spin. The yrast and partner bands are separated by ~ 200 keV at spin 12 and 400 keV at spin 16. This is a little less than the situation observed experimentally, where the energy gap is ~ 550 keV up to spin 14 and ~ 450 keV at $I^\pi = 15^-$. In principle the chiral bands should attain degeneracy at a certain spin; however, until now this has been observed only in the two odd-odd cases (^{104}Rh and ^{134}Pr). The present case of ^{100}Tc comes in the same category as the majority of the cases where the two bands do not attain degeneracy within the known spins. The reasons for this are not fully understood and further theoretical work is clearly required to explain this feature.

The next important parameter, which is a key signature of chirality, is the small amplitude of staggering (or no staggering at all in the ideal case) of the parameter $S(I)$, defined as $S(I) = [E(I) - E(I-1)]/2I$. The value of $S(I)$

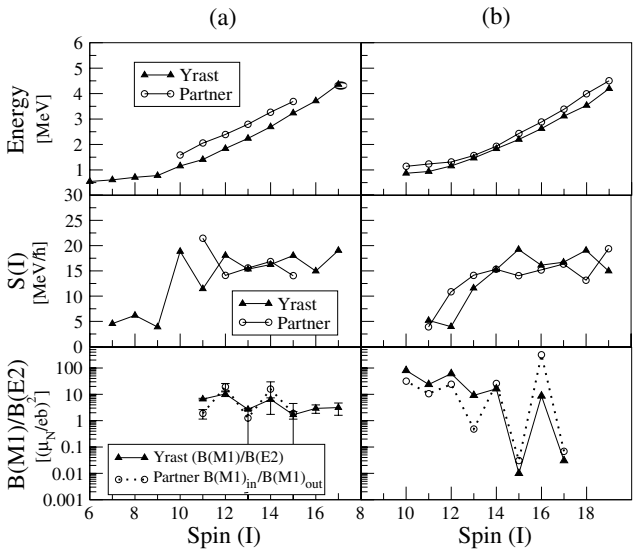

Fig. 5. Plot of the excitation energy *vs.* spin (I) (top), staggering $S(I) = [E(I) - E(I-1)]/2I$ (middle) and the $B(M1)/B(E2)$ ratios for the yrast and partner band as well as the $B(M1)_{\rm in}/B(M1)_{\rm out}$ ratios for the partner band (bottom). These are shown for: (a) experimental data, (b) particle plus rotor model calculations. The same symbols have been used for experimental as well as theoretical results.

shows large staggering in the odd-odd nuclei where the rotation is confined in the plane containing the spin vectors of the odd particles. This is due to the effect of the Coriolis force, which is proportional to the dot product of the collective angular momentum vector with the vectors of the single-particle spins. The unique situation in the case of chiral rotation, where the collective angular momentum vector is perpendicular to the angular momentum vectors of the odd particles, gives rise to a vanishing dot product of these vectors and therefore results in a highly reduced staggering amplitude. The middle panels of fig. 5(a) and (b) show the experimental and the calculated values of $S(I)$, respectively. It is clear from the figure that the situation in ^{100}Tc indeed favours a triaxial rotation in which the Coriolis force is minimum, thereby giving rise to a reasonably smoothly varying $S(I)$ parameter value. The bottom panels of fig. 5 show the experimental and calculated transition probability ratios $B(M1)/B(E2)$ for the yrast band and $B(M1)_{\rm in}/B(M1)_{\rm out}$ values for the partner band. The values in this panel are also presented in table 2. Evidence for staggering is seen in these ratios. Furthermore, the odd spin values are found to be staggered lower in magnitude compared to the even spins in both cases. This staggering, which is the third characteristic of the chiral phenomenon, is related to the spin and parity of the individual states in such a way that for odd-parity configurations, the odd spins are expected to be staggered lower, whilst the even spins are staggered higher. Both the experimental as well as the calculated staggerings for ^{100}Tc shown in the bottom of fig. 5 indicate that ^{100}Tc fulfils the third characteristic expected from chiral structures.

Table 2. Experimental $B(M1)/B(E2)$ values for the transitions in the yrast band and $B(M1)_{\rm in}/B(M1)_{\rm out}$ values for the transitions in the partner band, observed in ^{100}Tc alongwith the theoretical values calculated using the quasi-particle plus rotor model. See bottom panel of fig. 5. for the plots.

Spin	$B(M1)/B(E2)$		$B(M1)_{\rm in}/B(M1)_{\rm out}$	
I^π	Experiment $(\mu_N/eb)^2$	Theory $(\mu_N/eb)^2$	Experiment	Theory
10^-				31.52
11^-	6.6(6)	23.74	1.9 (7)	10.64
12^-	10.3(21)	61.21	19.6 (63)	24.04
13^-	2.7(2)	9.15	1.3(15)	0.48
14^-	6.4(9)	16.27	15.7(140)	25.85
15^-	1.7(5)	0.01	1.9(26)	0.03
16^-	2.9(10)	8.67		316.58
17^-	3.1(15)	0.03		0.07

Recently, Koike *et al.* [28] suggested that the ratios $B(M1)_{\rm yrast}/B(M1)_{\rm partner}$ and $B(E2)_{\rm yrast}/B(E2)_{\rm partner}$ should be close to unity for the chiral bands. This implies that the $B(M1)/B(E2)_{\rm yrast}/B(M1)/B(E2)_{\rm partner}$ ratio should also be approximately equal to unity for pairs of chiral bands. Thus, the observation of the $E2$ transitions in the new side band and hence a measurement of the $B(M1)/B(E2)$ ratios for this structure in ^{100}Tc will be useful in providing further support to the concept of chirality in this nucleus.

4 Summary

In summary, the yrast and non-yrast negative-parity levels of ^{100}Tc were studied up to $I^\pi = 16^-$, (tentatively 17^-) and $I^\pi = 14^-$ (tentatively 15^-), respectively. This was carried out using the ^{96}Zr(^{7}Li, 3n)^{100}Tc reaction at a beam energy of 27 MeV and the six detector array at Stony Brook. The new, non-yrast, band decays into the yrast band through predominantly $M1$ transitions. The two bands have been found to exhibit the characteristic properties expected from a chiral vibrator. The macroscopic-microscopic calculations reveal the triaxial nature of the shape of this nucleus. In addition, quasiparticle plus triaxial rotor model calculations were performed to calculate the energy levels and the $B(M1)$ and $B(E2)$ values for transitions between the levels. The calculated $B(M1)/B(E2)$ ratios compare reasonably well with corresponding experimental values in the the yrast band. Furthermore, the calculated staggering for this band and the $B(M1)_{\rm in}/B(M1)_{\rm out}$ values for the $M1$ transitions within and coming out of the excited band show good agreement with the phase observed in the experimental data for these two quantities. A comparison with the other odd-odd chiral nuclei currently known in this mass region shows a similarity in each case of two of the key features expected from a chiral configuration; namely a smoothly varying $S(I)$ parameter as a function of spin and the staggering of the $B(M1)/B(E2)$ and $B(M1)_{\rm in}/B(M1)_{\rm out}$ values. These two signatures appear to provide a more robust

test of the chirality compared to the energy degeneracy criterion for the two bands, which has so far only been observed in ^{104}Rh in the $A \sim 100$ region. However, more theoretical work is needed in order to understand the reasons why the two bands fail to achieve degeneracy in the majority of the chiral cases discovered to date (note, a similar situation is found to exist in the $A \sim 130$ region, where at present only ^{134}Pr is found to have states that approach true degeneracy). This might include further investigation of the role of pairing and the presence of a γ-soft core on the energy separation between the two bands.

This work has been partially supported by the UK EPSRC and the US NSF under contract number PHY-0245018.

References

1. S. Frauendorf, J. Meng, Nucl. Phys. A **617**, 131 (1997).
2. V. Dimitrov *et al.*, Phys. Rev. Lett. **84**, 5732 (2000).
3. C.M. Petrache *et al.*, Nucl. Phys. A **597**, 106 (1996).
4. K. Starosta *et al.*, Phys. Rev. Lett. **86**, 971 (2001).
5. T. Koike, K. Starosta, C.J. Chiara, D.B. Fossan, D.R. LaFosse, Phys. Rev. C **63**, 061304 (2001).
6. R.A. Bark, A.M. Baxter, A.P. Byrne, G.D. Dracoulis, T. Kibedi, T.R. McGoram, S.M. Mullins, Nucl. Phys. A **691**, 577 (2001).
7. D.J. Hartley *et al.*, Phys. Rev. C **64**, 031304 (2001).
8. K. Starosta, T. Koike, C.J. Chiara, D.B. Fossan, D.R. LaFosse, Nucl. Phys. A **682**, 375c (2001).
9. T. Koike, K. Starosta, C.J. Chiara, D.B. Fossan, D.R. LaFosse, Phys. Rev. C **67**, 044319 (2003).
10. A.A. Hecht *et al.*, Phys. Rev. C **63**, 051302R (2001).
11. D.L. Balabanski *et al.*, Phys. Rev. C **70**, 044305 (2004).
12. C. Vaman, D.B. Fossan, T. Koike, K. Starosta, I.Y. Lee, A.O. Macchiavelli, Phys. Rev. Lett. **92**, 032501 (2004).
13. T. Koike *et al.*, *Frontiers of Nuclear Structure, Berkeley, 29 July - 2 August, 2002*, AIP Conf. Proc. **656**, 160 (2003).
14. C. Vaman *et al.*, private communications.
15. P. Joshi *et al.*, Phys. Lett. B **595**, 135 (2004).
16. J. Timar, *et al.*, Phys. Lett. B **598**, 178 (2004).
17. D.C. Radford, Nucl. Instrum. Methods A **361**, 297 (1995).
18. K.S. Krane, R.M. Steffen, R.M. Wheeler, Nucl. Data Tables A **11** 351 (1973).
19. K.O. Zell, H. Harter, D. Hippe, H.W. Schuh, P. von Brentano, Z. Phys. A **316**, 351 (1984).
20. A.M. Bizzeti-Sona, P. Blasi, A.A. Stefanini, G. Maino, A. Ventura, Z. Phys. A **352**, 247 (1995).
21. A. Gizon *et al.*, Eur. Phys. J. A **2**, 325 (1998).
22. H.J. Chantler *et al.*, Phys. Rev. C **66**, 014311 (2002).
23. T.R. Werner, J. Dudek, At. Data Nucl. Data Tables **59**, 1 (1995).
24. T.R. Werner, J. Dudek, At. Data Nucl. Data Tables **50**, 179 (1992).
25. K. Starosta *et al.*, Phys. Rev. C **65**, 044328 (2002).
26. A. Klein, P. Protopapas, S.G. Rohozinski, K. Starosta, Phys. Rev. C **69** 034338 (2004).
27. M.A.J. Mariscotti, G. Scharff-Goldhaber, B. Buck, Phys. Rev. **178**, 1864 (1969).
28. T. Koike, K. Starosta, I. Hamamato, Phys. Rev. Lett. **93**, 172502 (2004).